A publication of
The Williamsburg BioProcessing Foundation

January/February 2004

BioProcessing™ JOURNAL

Advances & Trends In Biological Product Development

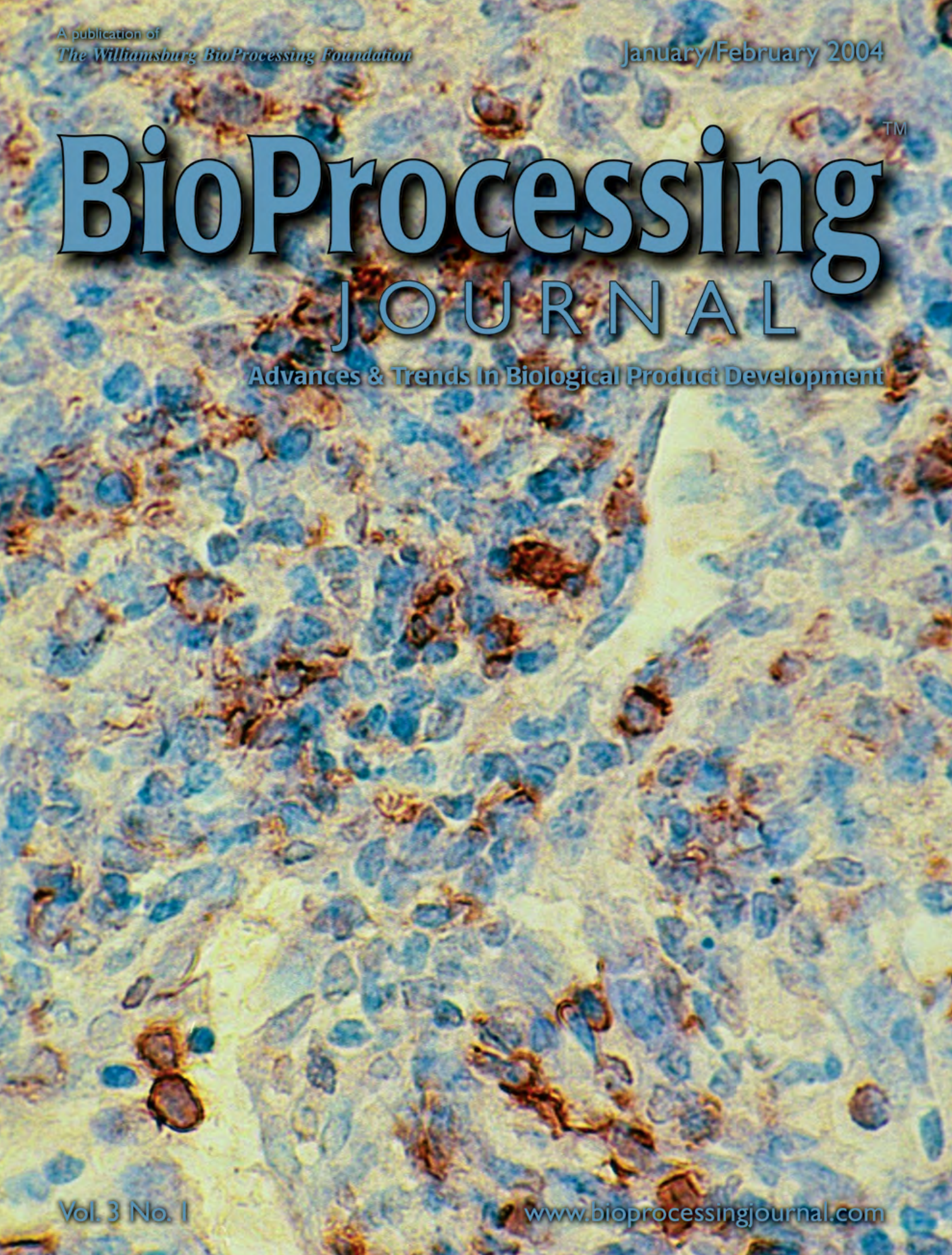

Vol. 3 No. 1

www.bioprocessingjournal.com

Optimisation of Virus Stock Production and Cell Infection Conditions for Protein Expression

By LOÏC GLEZ, CHRISTOPHE LOSBERGER, and THIERRY BATTLE

Variation of viral titre and recombinant product yields reported for the baculovirus expression vector system have been attributed to many specific infection variables.[1,2] These include multiplicity of infection (MOI) and cell density at time of infection and time of harvest, as well as virus bank quality and efficiency. The MOI is defined as the number of plaque forming units (pfu) per cell that are added at the time of infection. Virus titre (pfu/ml) is determined by the plaque assay method. The MOI parameter is easily manipulated and may be important in optimising recombinant protein yields. Other sources of variation during both cell growth and viral infection phases may be responsible for the range of reported yields. Past studies in our laboratory compared the behaviour of cells infected with high and low MOI values, specifically regarding nutrient limitation and deprivation.[3] In addition to these aspects, the quality of the virus bank may be an important factor which influences heterologous protein yields in the insect cell baculovirus system. Thus, production yields may be correlated to virus efficiency.

Although it is interesting to study the direct and indirect effects of MOI on recombinant protein production, we wanted to extend our analysis to the upstream events of virus stock production. Therefore, the parameters of viral stock generation were investigated for the optimisation of the infection conditions for expression of a recombinant protein, choosing ADAM17 as our reference protein.[4]

Materials & Methods

Cell Cultures and Medium

The insect cell *Spodoptera frugiperda* clone 9 line (Sf9, Invitrogen Corp., Carlsbad, CA) was employed to generate recombinant baculovirus stocks. The Sf9 cell line was cultured in SF900II serum-free medium (Gibco, Invitrogen). The insect cell *Spodoptera frugiperda* IPLB-21-AE line (Sf21 cells, Invitrogen) was dedicated to the virus titration by the plaque assay technique. The Sf21 cell line was cultured in TC100 medium (Gibco, Invitrogen) supplemented with 10% fetal calf serum (FCS) (JRH Biosciences Inc., Andover, Hampshire, UK), 0.1% Pluronic F-68 (Gibco, Invitrogen). One hundred ml of the two different insect cell line cultures were maintained at 27° C in 300-ml shaker flasks (Corning Inc., Corning, NY) at 170 rpm.

Recombinant Baculovirus

We investigated proprotein maturation by studying the processing of the recombinant human tumor necrosis factor alpha (TNF-α)-converting enzyme (TACE/ADAM17). Different cDNAs were studied and a specific truncated human ADAM17 (Met1–Arg473) including the signal peptide, the pro-domain, and the catalytic domain followed by a 6His tag was selected.[4] The construct contains the furin recognition motif at the junction between the pro-region and the catalytic domain. The furin

Loïc Glez is a biotech engineer; Christophe Losberger is an assistant scientist; and ***Thierry Battle, Ph.D.*** *(thierry.battle@serono.com) is head of protein expression, Serono Pharmaceutical Research Institute, Geneva, Switzerland.*

convertase activity results in production of the catalytic domain secreted (predicted molecular weight, 28 kDa) from its precursor form (predicted molecular weight, 54.8 kDa).

Virus Titre Determination

To determine and follow the extracellular viral titre of a specific type of baculovirus, the plaque assay technique was performed. When Sf21 cultures reached 80% confluency in a 6-well plate (2 x 10^6 cells/well), the growth medium was removed and 500 µl of viral solution, prepared at various serial dilutions, were added to each well. After two hours at 27° C, the virus was removed from the wells by aspiration. The wells were overlaid with 2 ml of a 1:1 preparation of 3% low-melting agarose/medium supplemented with 20% FCS. The cultures were incubated for three hours and the cell layer was covered with 1 ml of medium supplemented with 10% FCS. The cultures were incubated at 27° C for four days. Plaques were analysed by neutral red staining. After removal of the supernatant, each well was stained with 1 ml of 5% neutral red solution in sterile phosphate-buffered saline (PBS). Cultures were incubated for two hours at 27° C. Finally, after removal of the staining solution and destaining by inverting the plates for two hours, the number of infected spots per well appeared as clear white plaques on the red background. The pfu was calculated from data obtained in triplicate experiments.

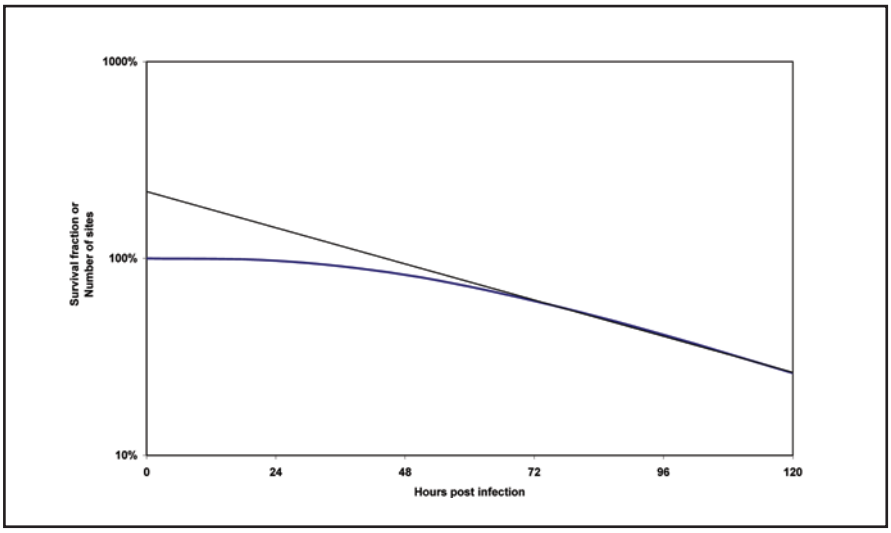

Figure 1. Survival curve predicted by the *n*-target theory. The *extrapolation number* (*n*) is determined by extrapolating the first-order portion of the survival curve to the *y*-axis, in this case, *n*=10.

Infection Experiments

Wild-type *Autographa californica nuclear polyhedrosis* virus (AcMNPV) and recombinant baculovirus encoding ADAM17 were amplified in the Sf9 cells. All experiments were performed using an original single viral batch, in the range of 10^8 pfu/ml. Cells to be used for infection were infected in the exponential growth phase at a cell density of approximately 1.1–1.3 x 10^6 viable cells/ml. The amount of virus added to the cells was based on the MOI specified in each experiment.

Cell Viability and Cell Counting

Cell viability was determined by the trypan blue dye exclusion method. The survival fraction was determined by the ratio of viable to total (viable and dead) cells.

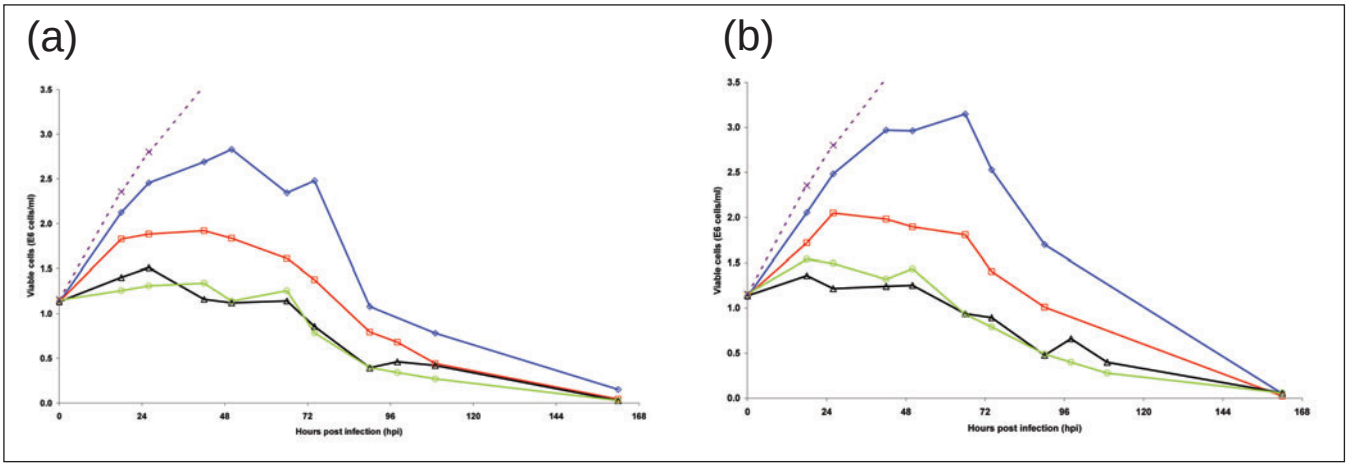

Figure 2. (a) Viable cell density of cultures infected with different MOIs of wild-type virus. Viable cells (10^6 cells/ml) were plotted compared to hours post infection (hpi). Control: uninfected cells (purple crosses). MOI values used were: 0.01 (blue diamonds), 0.1 (red squares), 1 (black triangles) and 10 (green circles). Infection started at 1.2 x 10^6 cells/ml. (b) Viable cell density of cultures infected with different MOIs of recombinant virus. Viable cells (10^6 cells/ml) were plotted compared to hours post-infection (hpi). Control: uninfected cells (purple crosses). MOI values used were: 0.01 (blue diamonds), 0.1 (red squares), 1 (black triangles) and 10 (green circles). Infection started at 1.2 x 10^6 cells/ml.

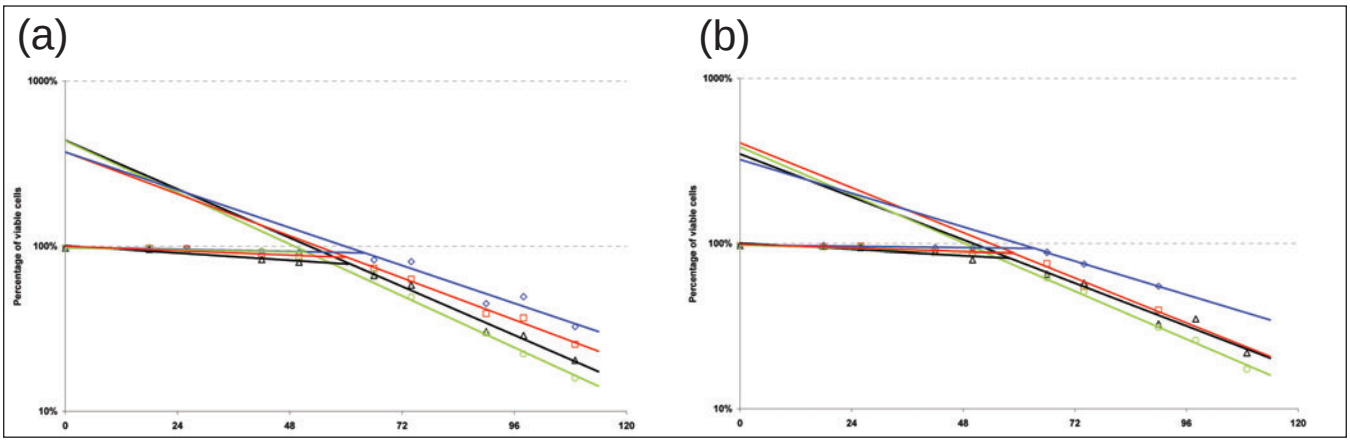

Figure 3. (a) Cell viability of cultures infected with varying MOIs of wild-type virus. Viable cells (10^6 cells/ml) were plotted compared to time post-infection (hpi). MOI values used were: 0.01 (blue diamonds), 0.1 (red squares), 1 (black triangles) and 10 (green circles). Infection started at 1.2 x 10^6 cells/ml. (b) Cell viability of cultures infected with varying MOIs of recombinant virus. Viable cells (10^6 cells/ml) were plotted compared to time post-infection (hpi). MOI values used were: 0.01 (blue diamonds), 0.1 (red squares), 1 (black triangles) and 10 (green circles). Infection started at 1.2 x 10^6 cells/ml.

n-*target Theory*

The *n*-target theory model was used to quantify cell death.[5,6] This model was originally derived to explain the survival rate of cells upon irradiation.[7–9] It assumes that each cell contains *n* inactivation sites, each of which must be hit at least once if the organism is to be inactivated. Moreover, two hits on one site are not more effective than one hit on a single site. The probability of a target to receive a hit is assumed to follow a Poisson distribution, because the success rate of hits is small and the number of hits is large. In baculovirus-infected insect cells, the hit is assumed to come from virus-derived factors. The cell viability is described by

$$V = (1\text{-}e^{-kt})^n$$

This equation explains the shoulder commonly seen in cell survival curves after irradiation (Fig. 1). At large values of *t*, it reduces to an equation:

$$\log(V) = \log(n) - kt$$

Therefore, the number of inactivation targets, *n*, is determined by extrapolating the first order portion of the survival curve to the *y*-axis. The *k* value can be determined from the slope in the first-order region (Fig. 1). Because this is a highly simplified model of cell death, the term *extrapolation number* has been proposed rather than number of inactivation targets.[9]

Gel Electrophoresis and Western Blots

One ml of sample culture was centrifuged at 2,000 x *g* for 10 minutes. One ml supernatant was retained and the cell pellets were frozen and resuspended in 1 ml H_2O. Recombinant 6xHis-tagged products were visualised by enhanced chemiluminescence Western blotting using rabbit monoclonal anti-His antibodies (Santa Cruz Biotechnology, Santa Cruz, CA) coupled to peroxidase-conjugated anti-rabbit immunoglobulin (DAKO A/S, Copenhagen, Denmark).

Results

Sf9 cells were infected with either wild type or recombinant ADAM17 baculovirus at the same time in parallel experiments.

Effects of Virus on Cell Growth and Viability

Effects of MOI on the Sf9-baculovirus system were studied by infecting cells at a variety of MOI ranging from 0.01 to 10 with infection during the growth phase at the cell density of 1.2 x 10^6 cells/ml (late-exponential phase). Both cell density and cell viability were shown to be strongly dependent on MOI (Figs. 2a and 2b). For both wild-type and recombinant virus, cell growth inhibition directly correlated with MOI. The post-infection growth curves of baculovirus-infected Sf9 cells grown in shaker flasks is shown in Figures 2a and 2b. At low MOI (0.01), cell density reached a maximum of 3 x 10^6 viable cells/ml. During the first 24 hours post-infection (hpi), the growth rate was only slightly lower than the uninfected growth rate, where uninfected cells usually reach densities above 6 x 10^6 viable cells/ml. This was probably due to a high number of uninfected cells. At a MOI of 0.1, the growth rate was rapidly limited and cessation of cell growth was observed at 48 hpi. Comparable growth inhibition was observed using MOI of 1 and 10. Cell growth was arrested early during the first 24 hpi and viable cell density declined earlier than with a MOI of 0.1.

Slight differences between the effects of wild-type and recombinant baculovirus on cell growth were observed in these two experiments. We used the n-target theory as a convenient means to evaluate these results and describe the effects of MOI and virus type on post-infection cell viability.

n-*target Theory Kinetic Characterization*

For both wild-type and recombinant virus, the rate of decrease in cell viability correlated with the MOI, where the

highest MOI gave the most rapid decrease. *n* and *k* values were determined from viability curves (Figs. 3a and 3b) by fitting the first order region to a straight line. The *y*-intercept is the *n* value, and the slope of this line is the *k* value. The results are summarized in Tables 3a and 3b. Survival curves showed that a decrease in MOI prolonged cell viability, increasing t_d and $t_{1/2}$, resulting in delayed cell death and a lower death rate. Increasing *k* values confirmed that use of increasing MOIs tended to speed up the cell death process. Extrapolation of all survival curves to the *y*-axis showed that the extrapolation numbers remained approximately the same (n=4, based on the *n* target theory) independent of wild-type or recombinant virus and of the MOI used.

MOI and Evolution of Viral Titre

The effect of MOI on virus generation was studied by infecting cells at four MOI values ranging from 0.01 to 10 with infection during the growth phase at the cell density of 1.2 x 10^6 cells/ml (late-exponential phase). Whatever MOI was used, it was observed that all eight virus generations reached the same extra-cellular virus titre between 48 and 72 hpi (Figs. 4a and 4b). Evolution of extra-cellular virus titre correlated with MOI, where the lowest MOI gave the most rapid increase. During the first 18 hpi, extra-cellular virus titre decreased by half, probably corresponding to the primary infection and first virus adsorption in the insect cells. Whatever the culture and MOI used, the virus titre increased until it reached the same maximum in the range of 10^8–10^9 pfu/ml. Wild-type virus infection resulted in a higher extra-cellular virus titre (6.8 x 10^8 on average) than recombinant virus (1.3 x 10^8 on average).

Optimisation of Baculovirus MOI and Recombinant Protein Production Yield

The effect of MOI on secreted recombinant protein was also studied in parallel to the effects on the extra-cellular recombinant virus titre evolution. Sf9 cells were infected with recombinant ADAM17 baculovirus at various MOIs, and then harvested at 72 hpi after which cell viability became too low and the degradation rate increased (data not shown). ADAM17 expression at different MOIs were analysed by Western blots (Fig. 5, 72 hpi).

Increasing the MOI resulted in an increase in ADAM17 expression. The secreted mature ADAM17 migrated as two bands of 34 and 38 kDa, which are slightly larger than predicted molecular weight (28 kDa), but consistent with the low mobility frequently observed with proteins of the ADAM variety under reducing conditions. The secreted mature ADAM17 was generated within all four MOI envisaged. Significant levels of the precursor ADAM17 form were clearly visible in the supernatant at MOI 10. Interestingly, at MOIs 1.0 and 10, precursor and mature secreted material were clearly visualised as doublets, whereas at MOIs of 0.01 and 0.1 only single bands were observed.

Table 3a. Kinetic characteristics of wild-type virus-induced cell death

Cell line	Baculovirus	MOI (pfu/cell)	t_d (h)	$t_{1/2}$ (h)	n	k ($10^{-2}h^{-1}$)
Sf9	Wild Type	0.01	64	31.5	4	2.2
Sf9	Wild Type	0.1	62	28.4	4	2.4
Sf9	Wild Type	1	59	24.5	4	2.8
Sf9	Wild Type	10	52	23.1	4	3.0

Table 3b. Kinetic characteristics of recombinant virus-induced cell death

Cell line	Baculovirus	MOI (pfu/cell)	t_d (h)	$t_{1/2}$ (h)	n	k ($10^{-2}h^{-1}$)
Sf9	Recombinant	0.01	66	35.4	4	1.9
Sf9	Recombinant	0.1	59	26.6	4	2.6
Sf9	Recombinant	1	58	27.8	4	2.5
Sf9	Recombinant	10	53	24.8	4	2.8

Discussion

Within the *n*-target theory of infected cell death kinetics, the extrapolation number is assimilated to the number of inactivation targets per cell.[9] In our experiments, this remained constant at n=4 independent of the MOI studied for both wild-type and recombinant infections that were analogous in behaviour. Moreover, proportionality between t_d and $t_{1/2}$ demonstrated that the cell death process was affected by only one common factor under the conditions investigated: MOI, independent of whether wild-type or recombinant virus were used. Cell death rates (*k* values) of infected cells were directly correlated to the MOI used for infection. This confirms that virus infection was responsible for the insect cell death process. Thus, the use of high MOIs tended to speed up the process of cell death. Survival curves showed that a decrease in MOI prolonged cell viability, causing delayed cell death and lower death rate. Cell growth and viability were shown to be directly correlated to the MOI, where the lower MOI resulted in better growth and cell viability. Nevertheless, and again independent of the starting MOI, a period of unaffected cell growth rate was observed during the first day post-infection. During this time frame the extra-cellular virus titre decreased. The first round of virus progeny release can explain both observations. Furthermore, this is supported by a recent study describing virus particles capable of binding within the first couple of hours

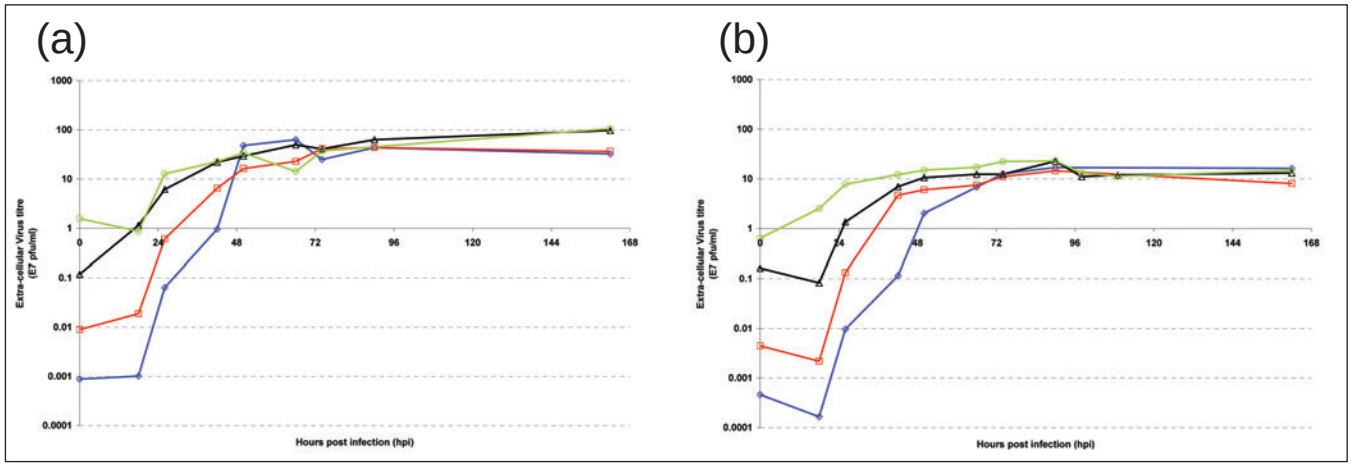

Figure 4. (a) Supernatant virus titre of cultures infected with different MOIs of wild-type virus. Virus titre (10^7 particles forming units/ml) was plotted compared to time post infection (hpi). MOI values used were: 0.01 (blue diamonds), 0.1 (red squares), 1 (black triangles) and 10 (green circles). Infection started at 1.2 x 10^6 cells/ml. (b) Supernatant virus titre of cultures infected with different MOIs of recombinant virus. Virus titre (10^7 particles forming unit/ml) was plotted compared to time post-infection (hpi). MOI values used were: 0.01 (blue diamonds), 0.1 (red squares), 1 (black triangles) and 10 (green circles). Infection started at 1.2 x 10^6 cells/ml.

in suspension culture.[10] The large proportion of uninfected insect cells contributed to the observed normal growth rate until the end of the first round of infection. At the MOI of 1, it is assumed that each cell was infected by at least one virus and entered the cell death process (accelerated at higher MOI).

Extra-cellular virus titre evolved independently of the MOI, and the same virus titre was reached after 72 hpi. Thus, it is of no benefit to delay the time of harvest after 72 hpi since the extra-cellular virus titre reaches a maximum independently of MOI. Whatever the starting MOI, for both wild-type and recombinant virus generation, high extra-cellular virus bank titres were obtained. The extra-cellular wild-type virus titre achieved was five times higher than that of the recombinant virus bank. The replacement of the polyhedrin by a recombinant protein may explain the lower extra-cellular recombinant virus titre detected. It was not obvious beforehand that a virus stock generated at different MOI would yield the same amount of virus particles (virus titre).

Because extra-cellular virus titre was shown to evolve independently of the MOI, it was of interest to study recombinant protein production. The recombinant protein product yield seemed to be higher when originating from cells infected using a high MOI. The n-target theory confirmed that when the *n* value remained constant, the protein expression was shown to be inversely correlated to the *k* values.[6] However, insect cell culture infected at a MOI of 10 secreted both the precursor and mature forms of ADAM17, yielding non-homogenous secreted material. Differential glycosylation could explain the different patterns observed for both precursor and mature ADAM17, as confirmed by a previous study.[11] Mature ADAM17 appeared as a doublet with apparent molecular weights of 34 and 38 kDa. This ADAM17 truncated construct shares the furin recognition motif at the junction between the pro-region and the catalytic domain. Furin's cleavage activity involves the predicted cleavage site Arg-Val-Lys-Arg214, but furin recognizes and cleaves after either the KR or RR dibasic sites.[12] Consistent with this hypothesis, two isoforms could be generated from the precursor form. Two mature protein series with different N-termini (Arg215 and Ala216) were probably generated, as demonstrated in a previous study.[13] The larger apparent molecular weights seen by SDS-PAGE must have resulted from inherent electrophoretic mobility characteristics of the polypeptides.

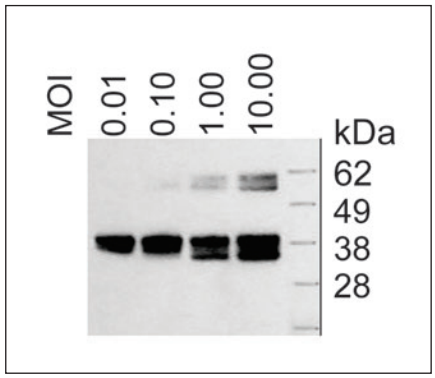

Figure 5. Western blot from cell supernatants at 72 hpi, infected at different MOI ranging from 0.01 to 10.

Finally, although recombinant protein yield was higher when originating from cells infected using high MOI, it contained large amounts of unprocessed protein. Lower MOI produced secreted material without detectable amounts of the precursor form.

Conclusion

Multiplicity of infection impacted directly on the behaviour of infected insect cells. Cell growth and cell viability were shown to be directly correlated to the MOI used — the lowest MOI resulted in maximal growth and cell viability. Extra-cellular virus titre evolved independently of the MOI; all the MOI tested resulted in the same

extra-cellular virus titre at 72 hpi. Therefore, there is no benefit in delaying the time of harvest longer than 72 hpi because the extra-cellular virus titre is already at its maximum. ADAM17 expression level was positively correlated to MOI, however, the use of low MOI produced more homogeneous material of the derived recombinant protein.

Although we cannot describe a specific relationship between the MOI used to generate virus stock and virus stock efficiency in generating recombinant proteins, this study helped to extend strategies in generating recombinant secreted proteins. Addressing virus generation conditions can be considered an approach to investigate virulence.

ACKNOWLEDGEMENTS

We would like to thank Dr. Amanda Proudfoot and Dr. Georg Feger for their helpful comments and careful proofreading of this manuscript.

REFERENCES

1. Blissard GW. Baculovirus–insect cell interactions. *Cytotechnology* 1996:20;73–93.
2. Licari P, Bailey JE. Factors influencing recombinant protein yields in an insect cell–baculovirus expression system: multiplicity of infection and intracellular protein degradation. *Biotech Bioeng* 1997:37;238–246.
3. Radford KM, Cavegn C, Bertrand M et al. The indirect effects of multiplicity of infection on baculovirus-expressed proteins in insect cells: secreted and non-secreted products. *Cytotechnology* 1997:24;73–81.
4. Moss ML, Jin SL, Becherer JD et al. Structural features and biochemical properties of TNF-alpha converting enzyme (TACE). *J Neuroimmunol.* 1997:72(2); 127–9.
5. Wu SC, Dale BE, Liao JC. Kinetics characterization of baculovirus-induced cell death in insect cell culture. *Biotech Bioeng* 1993:41; 104–110.
6. Wu SC, Jarvis DL, Dale BE et al. Heterologous protein expression affects the death kinetics of baculovirus-infected insect cell cultures: a quantitative study by use of n-target theory. *Biotechnol Prog* 1994:10; 55–59.
7. Condon EU, Terril HM. Quantum phenomena in the biological action of X-rays. *J Cancer Res* 1927:11; 324–333.
8. Atwood KC, Norman A. On the interpretation of recombinant proteins by baculovirus-infected gypsy moth cells. *Science* 1949:254; 1388–90.
9. Alper T, Gillies NE, Elkind MM. The sigmoid survival curve in radiobiology. *Nature* 1960:186;1062–63.
10. Rosinski M, Reid S, Nielsen LK. Kinetics of baculovirus replication and release using real-time quantitative polymerase chain reaction. *Biotech Bioeng* 2002:77(4);476–80.
11. Milla ME, Leesnitzer MA, Moss ML et al. Specific sequence elements are required for the expression of functional tumor necrosis factor-a-converting enzyme (TACE). *J Biol Chem* 1999:274;30563–70.
12. Hosaka M, Nagahama M, Kim WS et al. Arg-X-Lys/Arg-Arg motif as a signal for precursor cleavage catalysed by furin within the constitutive secretory pathway. *J Biol Chem* 1991:266–1217–30.
13. Clarke HR, Wolfson MF, Rauch CT et al. Expression and purification of correctly processed, active human TACE catalytic domain in *Saccharomyces cerevisiae. Protein Expr Purif.* 1998:13(1);104–10.

Can You Predict Your Future Research Needs?

With the Modular BioFlo® 110 Bioreactor You Don't Have To!

New Brunswick Scientific's BioFlo 110 Bioreactor/Fermentor lets you choose the system you need today, with the ability to easily upgrade as your requirements change.

- Pre-packaged kits with a wide range of add-on vessels, controllers, sensors & impellers allow easy system expansion.
- Designed for extremely simple operation: Large display uses "plain English" text to simplify setpoint control and monitoring.
- System is capable of regulating up to four vessels simultaneously.
- It's just one of a complete line of systems for research through production. Call for a free catalog today!

New Brunswick Scientific

Where Quality and Innovation Have Become Tradition

800-668-5040

Edison, NJ , USA• Fax: 732-287-4222 • bioinfo@nbsc.com

www.nbsc.com/wb

ANNUAL FDA SCIENCE FORUM 10th

FDA SCIENCE:

THE CRITICAL PATH

FROM CONCEPT TO CONSUMER

May18-19, 2004 • www.dcscienceforum.org

FDA WilBio AOAC INTERNATIONAL